

Effect of PTMGDA-PEGMA dopant on PVDF ultrafiltration membrane

Gui-E. Chen ^{*1}, Hui-Hong Huang ¹, Zhen-Liang Xu ²,
Ping-Yun Zhang ², Wen-Zhi Wu ¹, Li Sun ¹ and Yan-Jun Liu ¹

¹ School of Chemical and Environmental Engineering,
Shanghai Institute of Technology, 100 Haiquan Road, Shanghai 201418, China

² State Key Laboratory of Chemical Engineering, Membrane Science and Engineering R&D Lab,
Chemical Engineering Research Center, East China University of Science and Technology,
130 Meilong Road, Shanghai 200237, China

(Received October 24, 2015, Revised December 27, 2015, Accepted September 27, 2016)

Abstract. As a novel hydrophobic monomer, polytetrahydrofuran diacrylate (PTMGDA) was synthesized by the esterification reaction between polyethylene tetrahydrofuran (PTMG) and acryloyl chloride (AC). In situ free radical polymerization reaction method was utilized to fabricate poly(vinylidene fluoride) (PVDF)-PTMGDA-poly(ethylene oxide) dimethacrylate (PEGMA) ultrafiltration (UF) membranes. The performances of PVDF-PTMGDA-PEGMA UF membranes in terms of morphologies, mechanical properties, separation properties and hydrophilicities were investigated. The introduction of the PTMGDA-PEGMA dopants not only increased the membranes' pure water flux, but also improved their mechanical properties and the dynamic contact angles. The addition of the PTMGDA/PEGMA dopants led to the formation of the finger-like structure in the membrane bulk. With the increase concentration of PTMGDA/PEGMA dopants, the porosity and the mean effective pore size increased. Those performances were coincide with the physicochemical properties of the casting solutions.

Keywords: PVDF-PTMGDA-PEGMA membrane; PTMGDA-PEGMA dopants; in situ free radical polymerization; hydrophilicity

1. Introduction

PVDF has been used widely for the preparation of microfiltration (MF) membrane and UF membrane (Katsoufidou *et al.* 2005, Liu *et al.* 2011, Forsythe and Hill 2000) due to its excellent chemical resistance, exceptional hydrolytic stability, flexibility, thermal stability, oxidation resistance and mechanical properties (Yadav *et al.* 2010, Cui *et al.* 2014). However, the hydrophobic of the PVDF membranes limited its wide applications (Prince *et al.* 2014, Liu *et al.* 2013a). Consequently, the modification of PVDF membranes is of great importance. The important modification methods are surface and blending modifications. Current surface modification includes surface coating, plasma, and so on (Wang *et al.* 2002, Zuo and Wang 2013, Boributh *et al.* 2009, Li *et al.* 2013, Vähä-Nissi *et al.* 2012, Ulbricht and Belfort 1996, Kim *et al.*

*Corresponding author, Ph.D., E-mail: chengui@sit.edu.cn; chemxuzl@ecust.edu.cn

2009). However, the surface modifications only occur at the surface of the membrane, whereas, the stability of the modified membrane is relatively poor. Blending modification is a widely modification method, and high performance membranes could be obtained by using additives such as inorganic nanoparticles, hydrophilic polymers and amphoteric polymers (Li *et al.* 2012, Zhang *et al.* 2004, Letchford and Burt 2007, Zhang *et al.* 2009).

Recently, the application of amphiphilic polymers for PVDF membranes modification has attracted considerable attention. During the membrane formation process, the amphiphilic polymer used not only as an additive, but also as a modifier (Zhang *et al.* 2013a, b, Neugebauer 2007). The stability of the membrane is improved by the intertwining between the hydrophilic and hydrophobic regions of the amphiphilic polymer. Meanwhile, with the enrichment of the hydrophilic chain on the membrane surface, the hydrophilicity of the membrane improved. Liu *et al.* (2009) prepared hydrophilic and fouling resistant PVDF hollow fiber membranes via the blending method through the amphiphilic brush-like copolymer P(MMA-R-PEGMA) synthesized by atom transfer radical polymerization (ATRP) method. Hester *et al.* (1999) reported that the modification of PVDF membranes by blending poly(methyl methacrylate)-comb-poly(ethylene oxide) (PMMA-c-PEO), and a substantial surface enrichment of the comb polymer with hydrophilic nature was obtained. Loh *et al.* (2011) used the amphiphilic pluronic block copolymers to prepared high performance polyethersulfone UF hollow fiber membranes with improved the pure water permeation. Hashim *et al.* (Awanis Hashim *et al.* 2012) adopted in-situ grafting of PVDF-g-PEGMA to modify PVDF hollow fiber membranes with excellent hydrophilicity. Zhang *et al.* (2013a) modified PVDF membranes using the amphiphilic copolymer that synthesized via adding azodiisobutyronitrile (AIBN) into a PVDF-TEP-DMAc-PEGMA-MMA system to initiate the in situ free radical polymerization.

In this study, a novel hydrophobic monomer of PTMGDA is synthesized. Then PTMGDA works as hydrophobic reaction monomer, while PEGMA is chosen as hydrophilic reaction

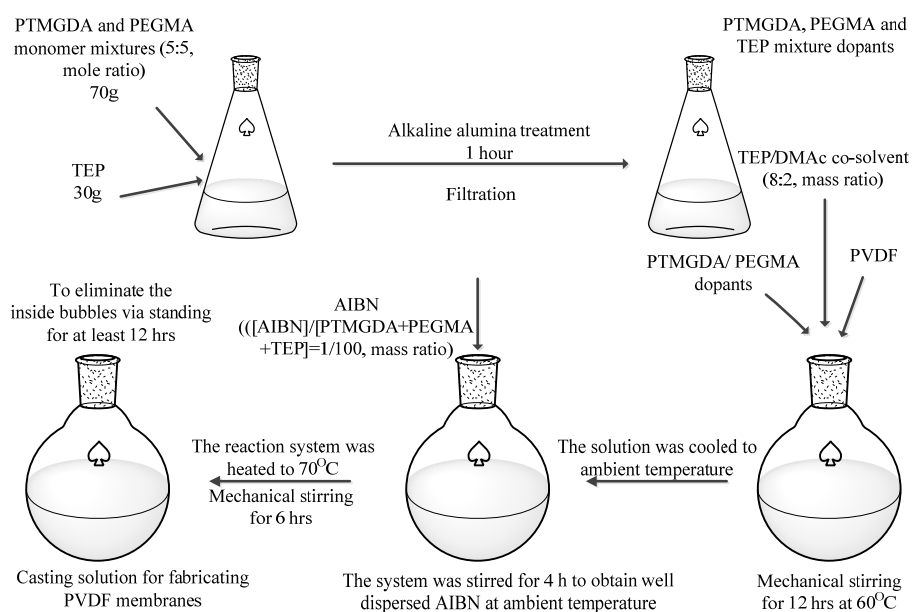


Fig. 1 Preparation diagram of PVDF casting solution

monomer. A PVDF casting solution is formed via an in situ free radical polymerization method by directly blending AIBN into the PVDF/PEGMA/PTMGDA/TEP/DMAc system. Then the casting solution is immersed into the deionized water to form PEGMA-PTMGDA-PVDF membranes via the non-solvent induced phase separation (NIPS) process (Yuan *et al.* 2008). The redundant or unreacted PTMGDA and PEGMA monomers worked as pore-forming agents are washed out during the phase separation process. The schematic diagram of PVDF membranes' preparation process of in situ free radical polymerization is shown in Fig. 1.

Using different contents of PTMGDA/PEGMA dopants, the properties of the casting solution and the performances of the PVDF membrane (mechanical properties, permeability performance, pore size distribution and hydrophilicity) are discussed.

2. Experimental

2.1 Materials

Polyoxytetramethylene (PTMG) and poly (vinylidene fluoride) (PVDF) were purchased from Department of Shanghai Chemical Industrial Co. Ltd (China) and Solvay Advanced Polymers, L.L.C (USA), respectively. Dichloromethane, hydrochloric acid, sodium chloride, hydroquinone, N, N-Dimethylacetamide (DMAc), Al_2O_3 and triethylamine were purchased from Sinopharm Chemical Reagent. Co., Ltd (China). Polyethylene glycol (PEG, $M_w = 1000, 4000, 6000, 10000, 20000$) and Albumin from bovine serum (BSA, $M_w = 67K$) were obtained from Sigma-Aldrich. Polyethylene glycol monomethyl ether methyl methacrylate (PEGMA, $M_n = 1200$) was obtained from Taijie chemical Co., Ltd (China, Shanghai). Triethyl phosphate (TEP) and azodiisobutyronitrile (AIBN) were purchased from Tansoole Chemical Co., Ltd (China). Acryloyl chloride and deionized water were prepared by our own lab.

2.2 Synthesis of PTMGDA monomer

The synthetic route of PTMGDA is shown in Fig. 2. 2 mol triethylamine, 1 mol PTMG and a small amount of hydroquinone were mixed with 200 ml dichloromethane in a 500 ml flask and placed in an ice bath. The solution was stirred and a mixed solution of dichloromethane and acryloyl chloride was slowly added by a constant pressure funnel, keeping the mole ratio of acryloyl chloride and triethylamine 1:1. The stirring was continued for 0.5 hr until the acryloyl chloride was dripped off. The mixture solution was then transferred to a 35°C water bath and stirred for 12 hrs. After that, the reaction solution was filtered to obtain a filtrate. The excess acryloyl chloride and triethylamine are removed by dilute hydrochloric acid. Then the pH was adjusted to 7.0 with a saturated aqueous sodium chloride solution. Anhydrous magnesium sulfate filtered and methylene chloride in the filtrate was removed by rotary evaporation at 35°C. Finally, the viscous liquid PTMGDA was obtained.

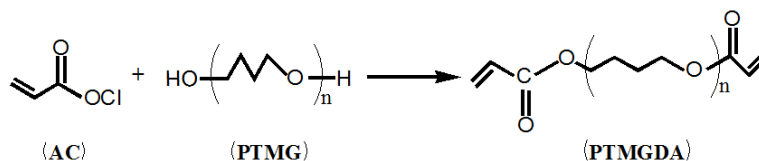


Fig. 2 The synthetic route of PTMGDA

Table 1 Compositions of the casting solutions

Membrane No.	PVDF (wt.%)	TEP/DMAc (wt.%)	PTMGDA-PEGMA-TEP (wt. %)	AIBN (wt. %)	Coagulant bath
MPTMGDA-PEGMA- 0	18.0	65.6/16.4	0.0	0.00	Water
MPTMGDA-PEGMA-1 ^a	18.0	64.8/16.2	1.0	0.00	Water
MPTMGDA-PEGMA-1	18.0	64.8/16.2	1.0	0.01	Water
MPTMGDA-PEGMA-2	18.0	64.0/16.0	2.0	0.02	Water
MPTMGDA-PEGMA-3	18.0	63.2/15.8	3.0	0.03	Water
MPTMGDA-PEGMA-4	18.0	62.4/15.6	4.0	0.04	Water
MPTMGDA-PEGMA-5	18.0	61.6/15.4	5.0	0.05	Water

^a 1.0wt.% PTMGDA / PEGMA/TEP mixture solution without polymerization

2.3 Preparation of PVDF-PEGMA-PTMGDA UF membranes

70 g PTMGDA-PEGMA (PTMGDA : PEGMA = 5 : 5, molar ratio) were dissolved in 30 g TEP in a 250 ml conical flask, containing 1.0wt.% alumina (basic). The solution was stirred for 1h and a homogeneous solution containing PEGMA, PTMGDA and TEP was obtained after filtration. The UF membranes were prepared via NIPS method (Khayet *et al.* 2002). In brief, the membranes were prepared from the casting solutions containing PVDF, PEGMA, PTMGDA, TEP and DMAc (8:2, mass ratio) according to the compositions listed in Table 1. These casting solutions were prepared in 250 ml conical flasks and heated to approximately 70°C while being mechanically stirred for 12 hrs. After the PVDF was completely dissolved, AIBN was added into the solution at room temperature. The solution was then heated to 70°C and mechanically stirred for 6 hrs. Afterward, the casting solution was degassed without stirring for 24 hrs at 70°C until gas bubbles were no longer visible. The casting solutions were cast on glass plates and immediately immersed in deionized water at 25°C. The membranes were left in the deionized water for one week and the deionized water was changed twice daily. Subsequently, the membranes were air-dried for 48 h.

2.4 Characterization

Characterization of PTMGDA monomer:

The chemical structure of PTMGDA was analyzed by ¹H-NMR (AVANCEIII 500 MHZ. Bruker Co., Germany) and FT-IR (Nicolet 6700 FT-IR spectrometer) for group characteristic chemical shift values and characteristic peak values, respectively. ¹H NMR spectra was recorded on a Bruker BioSpin GmbH (Germany) operated at 400 MHz, using D₆-DMSO and tetramethylsilane (TMS) as solvents and internal standard, respectively.

Surface tension: The surface tension of the casting solution was obtained by a JK99C Automatic Surface and Interface Tension Measure Instrument (Shanghai Zhongcheng Digital Technology Apparatus Co. Ltd., China) via the Wilhelmy plate method at 25°C.

Viscosity: The viscosities of the casting solutions were measured by a DV-II+PRO Digital Viscometer (Brookfield, USA) at 25°C, controlled by a water bath. The viscosity change was monitored with shear rate.

Dynamic light transmittance:

Dynamic light transmittance experiment was measured by a self-made device as described by

Liu *et al.* (2013b). The casting solution was cast on a glass plate and immersed in deionized water with a laser directed on the glass plate. The light intensity was recorded on the computer via a sensor. The dynamic light transmittance of the casting solution in the deionized bath was characterized by the curve of light transmittance with regard to immersion time.

Morphology:

The surface and cross-section membrane morphologies were observed with high resolution scanning electron microscopy (S-3400, Hitachi, Japan). The cross-sectioned samples were obtained by fracturing in liquid nitrogen and then sputter-coated with gold.

Mechanical properties:

The mechanical properties of the membranes were measured by using Microcomputer-Digital Display Integrative Control Testing Machine (QJ210A, Shanghai Qingji Instrument Sciences and Technology Co. Ltd., China). The sample of $15 \times 10 \text{ mm}^2$ is clamped and pulled at tensile rates of 50 mm/min at ambient temperature. To minimize experimental errors, the flat sample specimen was tested using 5 repeat measurements.

Dynamic contact angle (DCA):

The DCA of the membrane surfaces were measured with a contact angle analyzer (JC2000D1, Shanghai Zhongcheng Digital Technology Apparatus Co. Ltd., China). The apparatus was connected to a camera which started taking pictures when a water droplet of 20 μL was dispersed on the membrane surface. For each membrane, an average value was obtained by using 3 repeat measurements.

Filtration properties of the membranes:

The permeation flux (J_w), flux recovery ratio (FRR) and pore size distribution were measured by UF equipment. All experiments were controlled at 25°C with a constant pressure of 0.1 MPa. The permeation flux was measured after the membranes were pre-pressured with pure water at 0.1 MPa, and then, the pure water flux, the BSA flux, the flux recovery and the rejection rate R (%) for PEG (MW 1000, MW 4000, MW 6000, MW 10000, MW 20000) were measured according to the method described by Zhao *et al.* (2014). The concentration of PEG in the permeation and feed solutions were analyzed by a Ternary Optical Computer (TOC) analyzer (Shimadzu TOC-VCPH, Japan). The pore size distribution of the prepared membranes was measured in a 300 mg/L PEG (MW = 1000, 4000, 6000, 10000, 20000) solution by the UF experimental equipment. The mean pore size and weight cut-off (MWCO) of the prepared membranes were characterized by the method described in References (Yang *et al.* 2007).

The permeation flux (J_w), FRR (%) and the rejection rate R (%) are defined as Eqs. (1), (2) and (3), respectively (Yu *et al.* 2009).

$$J_w = \frac{V}{A \times t} \quad (1)$$

$$FRR = \frac{J_R}{J_w} \times 100\% \quad (2)$$

$$R = \left(1 - \frac{C_p}{C_f}\right) \times 100\% \quad (3)$$

Where J_W and J_R are the permeation fluxes of pure water and BSA solution ($L \cdot m^{-2} \cdot h^{-1}$), respectively; V is the volume of permeate pure water or BSA solution (L); A is the membrane area ($A = 2.826 \times 10^{-3} m^2$) and t is the permeation time (h). The C_p and C_f are the concentrations of PEG in the permeation and feed solutions, respectively.

The porosity (ε) of the membrane was measured by the dry-wet method as described by Chen *et al.* (2014), and the porosity is calculated experimentally by the Eq. (4)

$$\varepsilon = \frac{(m_{wet} - m_{dry}) / \rho_{water}}{(m_{wet} - m_{dry}) / \rho_{water} + m_{dry} / \rho_{pvdF}} \times 100\% \quad (4)$$

Where m_{wet} and m_{dry} are the weights of the wet and dried membranes, respectively; ρ_{water} and ρ_{pvdF} are the water density ($1.0 g/cm^3$) and the polymer density ($1.765 g/cm^3$), respectively.

The pore size distribution of the membrane is described using the most common form of the log-normal distribution function

$$f(d) = \frac{2}{\ln(\sigma)d\sqrt{2\pi}} \exp\left[-\frac{1}{2}\left(\frac{\ln(d/\mu)}{\ln(\sigma)}\right)^2\right] \quad (5)$$

Where the two parameters of μ and σ are the geometric mean diameter and the geometric standard deviation, respectively. The UF experiments method described by Yang *et al.* (Yang *et al.* 2007, Yu *et al.* 2009) is utilized to determine these two parameters and MWCO using 300 mg/L PEG (MW 1 kg/mol, MW 2 kg/mol, (Yang *et al.* 2005) experiment is carried out three times and the averaged values of results are utilized as the final ones to reduce the uncertainty. Besides, the pore size distribution parameters μ and σ are then obtained by minimizing the differences between the theoretical and experimental rejection values (Shi *et al.* 2008).

3. Results and discussion

3.1 1H -NMR and FT-IR Analysis of PTMGDA monomer

1H -NMR and FT-IR analysis was used to investigate the chemical component of the PTMGDA monomer. The 1H -NMR characteristic peaks of the PTMGDA monomer in spectra was shown in Fig. 3(a). The resonance $\delta = 1.0\sim 2.0$ ppm and $\delta = 3.0\sim 4.0$ ppm could be assigned to the H- of $-C-CH_2$ and $O-CH_2$ of PTMG, respectively. The $-CH = CH_2$ group in the acryloyl chloride segment indicated a chemical shift of $\delta = 5.5\sim 6.5$ ppm. Then the chemical structure of the PTMGDA monomer was further confirmed by FT-IR, which was shown in Fig. 3(b). Comparison of PTMG, the spectrum of PTMGDA indicated two new absorption peaks at $1620 cm^{-1}$ and $1720 cm^{-1}$, which were ascribed to the $C = C$ and $O - C = O$ of the acryloyl chloride, respectively. The FT-IR spectrum for PTMG and PTMGDA further demonstrated that the PTMGDA monomer had been synthesized successfully.

3.2 Physicochemical properties of the casting solutions

The surface tension results were shown in Fig. 4. The surface tension of pure PVDF in DMAc-TEP co-solvent is 31.92 ± 0.72 mN/M. Fig. 4 revealed that after the addition of the dopants, the surface tension decreased. It indicated that dramatically decreasing surface tension was ascribed to

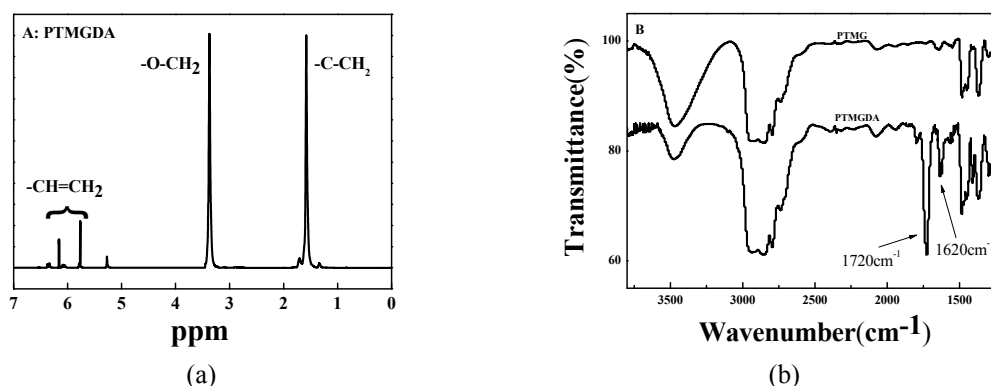


Fig. 3 (a) $^1\text{H-NMR}$ spectrum of PTMGDA; and (b) FT-IR spectrum of PTMG and PTMGDA

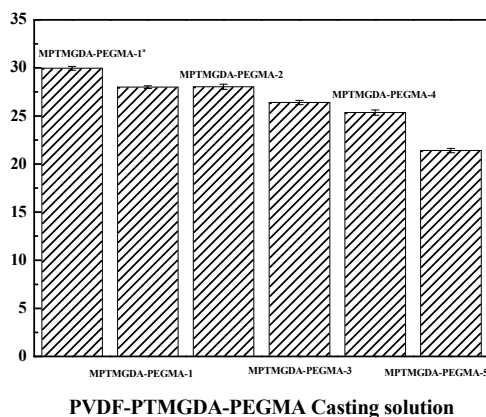


Fig. 4 The surface tensions of the casting solutions

the reaction of the hydrophobic and the hydrophilic monomer after in situ free radical polymerization. Furthermore, with increasing concentration of the dopants, the surface tension decreased from 28 mN/M to 19 mN/M. Reason behind that was the synthesis of amphiphilic polymer P(PTMGDA-*r*-PEGMA) after situ free radical polymerization. P (PTMGDA-*r*-PEGMA) was amphiphilic polymer, which led to the surface tension decreased. Furthermore, the surface tension was associated with the molecular recombination of the gas-liquid interface. Additionally, the decreasing surface tension illustrated the reaction of PTMGDA and PEGMA.

Viscosity could control the dynamics during membrane formation process, which influenced the morphology of membranes' surface and cross-section. The viscosity curves were shown in Fig. 5. Fig. 5 showed that all the casting solutions possessed the shear thinning. Compared with MPTMGDA-PEGMA-1^a, the viscosity increased after in situ free radical polymerization. The curves indicated that with the existence of the dopants, the intermolecular interactions of the casting solutions became weakened, the viscosity of the casting solution reduced from 4500 to 4000 cp. Furthermore, with an increasing content of the dopants, the viscosity of the casting solution increased from 4000 to 6500 cp. This could be attributed to the increase of PVDF-PTMGDA-PEGMA agglomerated, the strong intermolecular interactions between the molecular

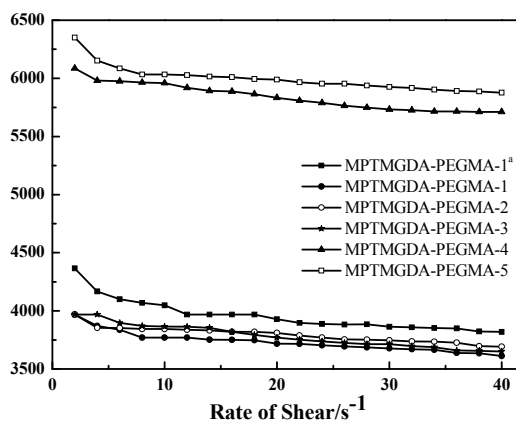


Fig. 5 Viscosity curves of the casting solutions

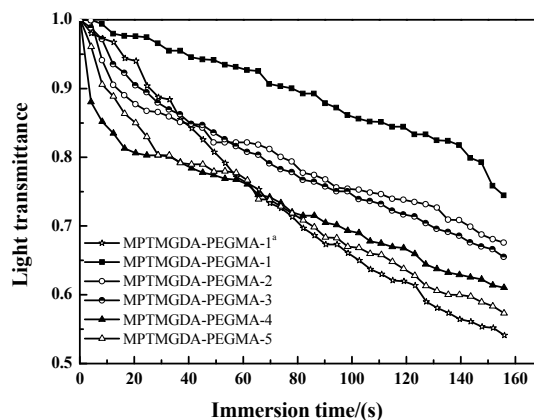


Fig. 6 The light transmittance curves of the casting solutions

contributed to the enhanced viscosity. Furthermore, it demonstrated that the strong intermolecular interaction of the PVDF casting solution reduced the chain stretching and movement.

The precipitation curves of Fig. 6 revealed that the precipitation rate of the casting solution without in situ free radical polymerization was the fastest of all. Besides, from Fig. 6, we could obtain that the in situ free radical polymerization contributed to the enhancement demixing process, and the casting solutions' precipitation rate increased as the concentration increasing of the PTMGDA-PEGMA-TEP dopants. Furthermore, all the curves indicated that liquid-liquid demixing occurred before the crystallization, and the MPTMGDA-PEGMA-4 and MPTMGDA-PEGMA-5 had the minimum time of the instantaneous demixing process. It is believed that the instantaneous demixing process resulted the formation of a dense skin layer in the membrane surface and a finger-like structure in the membrane bulk (Zhang *et al.* 2013c).

3.3 Morphologies and mechanical properties

As seen in Fig. 7, the surface of the pure PVDF membrane was smooth. Without in situ polymerization, the membrane morphologies show macro-pores surface for the monomer worked

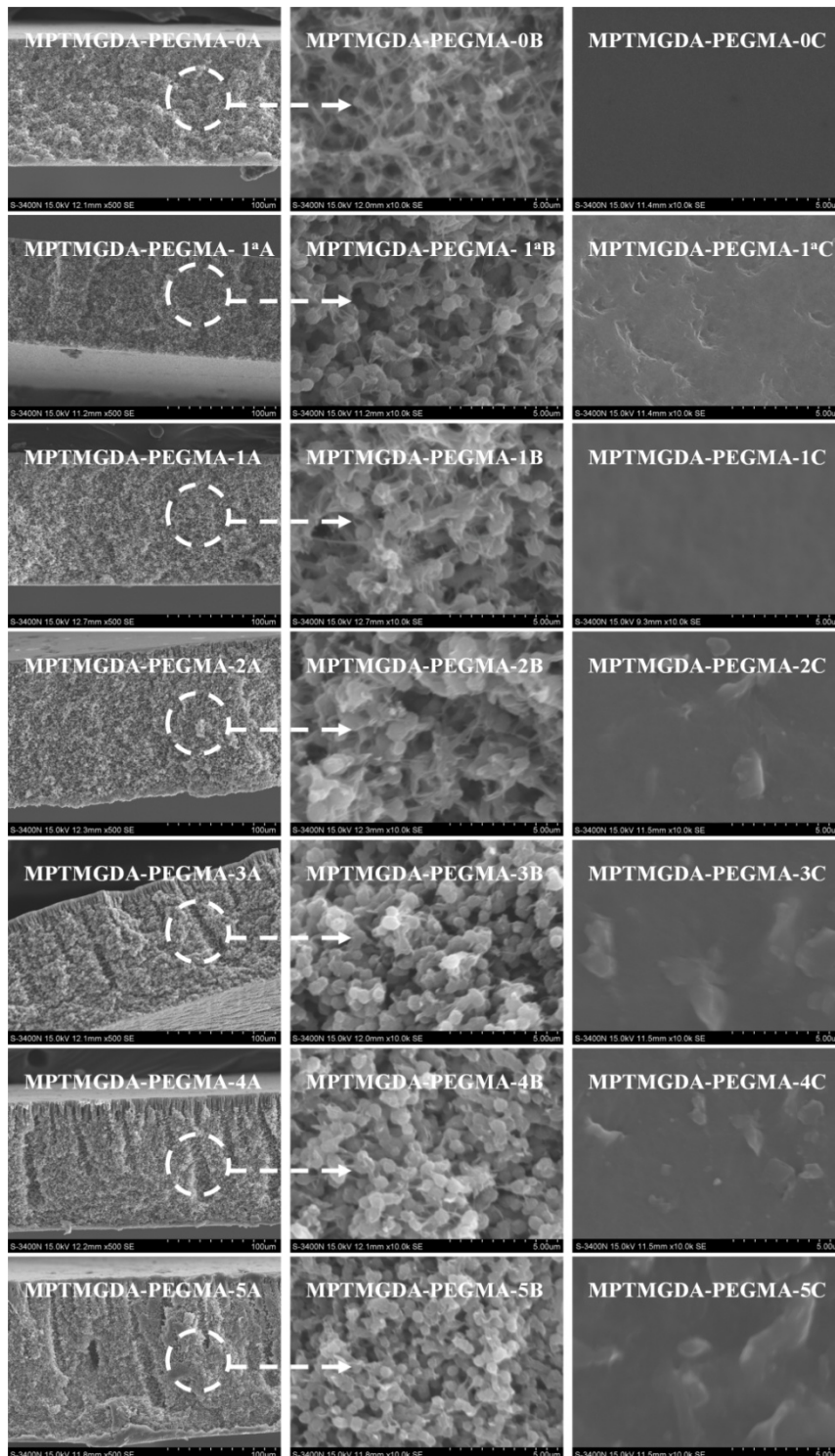


Fig. 7 SEM images of the cross-sections and the outer surface of PVDF-PEGMA-PTMGDA membranes (A-Cross section; B-Enlarged cross section; C-Outer surface)

as the pore-forming agent during demixing process. While after in situ free radical polymerization, the membranes showed dense layer. Besides, the pure PVDF membrane possesses just sponge-like structure, whereas, the other membranes showed both the finger-like and the sponge-like structure in the membrane bulk. The formation of the denser skin and finger-like structure might be caused by the instantaneous demixing process. In addition, Fig. 7 indicated that after in situ polymerization, the length of the finger-like structure abruptly shortened. What's more, the finger-like structures became more prominent with increased concentration of the PTMGDA-PEGMA-TEP dopants. It also could be observed that PVDF nanograins arranged in a form of spherical-sharp, then they were replaced by the cloud form after the in situ radical polymerization. And large voids appeared, those cloud form nanograins became spherical-sharp as increasing content of the PTMGDA-PEGMA-TEP dopants. These images were consistent with the result of the precipitation rate of the corresponding casting solutions.

The important parameters of the resultant membranes' mechanical properties were the break strength, elongation at break and Young's modulus. In Table 2, it showed that the Young's modulus firstly decreased and then increased after in situ free radical polymerization. As increasing concentration of the dopants, the elongation at break decreased from 157% of MPTMGDA-PEGMA-1 to 41.2% of MPTMGDA-PEGMA-5. This result could be explained by the enhanced length of the finger-like structures and the existed large voids in the membrane bulk. The existence of the PTMGDA monomer significantly improves the stiffness of the membranes.

3.4 Filtration performance

The J_w , J_B , FRR and the porosity of the resultant membranes are presented in Fig. 8 and Table 3, respectively. Notably, after the in situ free radical polymerization, the flux and FRR of the membranes decreased substantially. However, the J_w (from MPTMGDA-PEGMA-1 to MPTMGDA-PEGMA-5) increased from 25.1 L.m⁻¹.h⁻¹ to 60 L.m⁻¹.h⁻¹. Meanwhile, as increasing concentration of the dopants, the J_B increased from 10.8 L.m⁻¹.h⁻¹ of MPTMGDA-PEGMA-1 to 30.0 L.m⁻¹.h⁻¹ of MPTMGDA-PEGMA-5. Besides, as the dopants content increased from 1.0wt.% to 5.0wt.%, the FRR was up to 47.9%. These results were attributed to the structure of the resultant membranes. Though the increased porosity of Table 3 could increase the flux of resultant membranes to some extent, previous research believed that the dense skin contributed to the decreased flux (Zhang *et al.* 2012). However, combined with the SEM images, we found that the membranes possessed dense skin showed improved J_w , J_B and FRR. It is believed that the

Table 2 Mechanical properties of PVDF-PTMGDA-PEGMA membranes

Membrane No.	Break strength /MPa	Elongation at break /%	Young's modulus /MPa
MPTMGDA-PEGMA-0	4.4 ± 0.2	295 ± 3.8	89.8 ± 4.9
MPTMGDA-PEGMA-1 ^a	3.7 ± 0.4	161 ± 8.9	59.7 ± 5.6
MPTMGDA-PEGMA-1	3.9 ± 0.3	157 ± 7.1	51.6 ± 8.0
MPTMGDA-PEGMA-2	3.7 ± 0.6	105 ± 9.5	56.1 ± 6.8
MPTMGDA-PEGMA-3	2.9 ± 0.4	64.8 ± 6.5	61.9 ± 7.1
MPTMGDA-PEGMA-4	2.6 ± 0.1	58.5 ± 3.1	62.9 ± 11.4
MPTMGDA-PEGMA-5	2.6 ± 0.2	41.2 ± 4.1	87.9 ± 4.9

^a 1.0wt.% PTMGDA / PEGMA/TEP mixture solution without in situ free radical polymerization

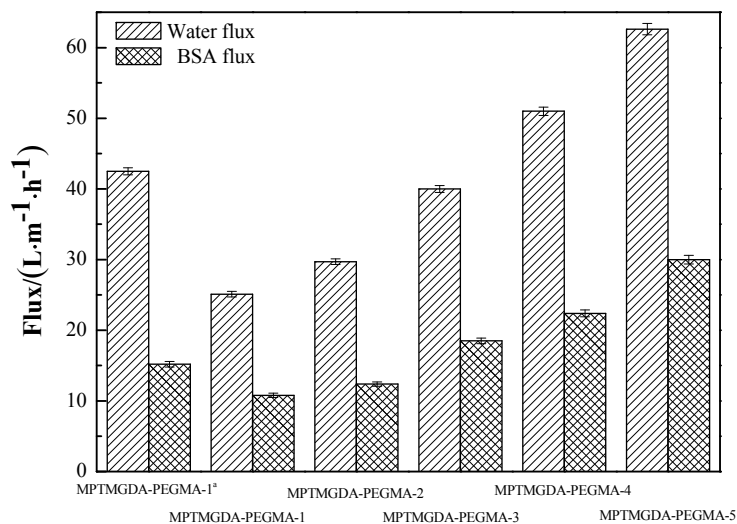


Fig. 8 Pure water fluxes and BSA fluxes of PVDF-PTMGDA-PEGMA membranes

Table 3 Mechanical properties of PVDF-PTMGDA-PEGMA membranes

Membrane No.	FRR/%	Porosity/%
MPTMGDA-PEGMA-1 ^a	35.5 ± 0.5	74.0 ± 0.8
MPTMGDA-PEGMA-1	43.0 ± 0.6	69.6 ± .9
MPTMGDA-PEGMA-2	41.8 ± 0.3	76.2 ± 1.1
MPTMGDA-PEGMA-3	46.3 ± 0.5	78.0 ± 1.5
MPTMGDA-PEGMA-4	43.9 ± 0.4	78.3 ± 1.3
MPTMGDA-PEGMA-5	47.9 ± 0.5	80.1 ± 1.6

^a 1.0wt.% PTMGDA / PEGMA/TEP mixture solution without polymerization

hydrophilic segments of the dopants after in situ polymerization explained the increased J_W , J_B and FRR. Zhang *et al.* reported that the hydrophilic segments of the amphiphilic copolymer would surface segregation during demixing process, which improved the hydrophilicity of resultant PVDF membranes, resulting improvement of J_W , J_B and FRR (Zhang *et al.* 2013a).

3.5 Pore size and molecular weight cut-off (MWCO)

The probability density function and the cumulative pore size distribution were presented in Figs. 9(a) and (b), respectively. The mean effective pore size and MWCO of the resultant membranes were shown in Table 4. With the increase of dopants, the pore size distribution becomes wider. After in situ free radical polymerization, the mean effective pore size decreased from 9.5 nm to 6.08 nm. This was ascribed to the reaction of the PTMGDA and PEGMA; the hydrophilic segment was segregation on the membrane surface. The high precipitation rate in Fig. 6 led to the enhanced finger-like structure and the large voids. Besides, the increased length of the finger-like structures with the increasing content of the dopants was coincide with the increasing

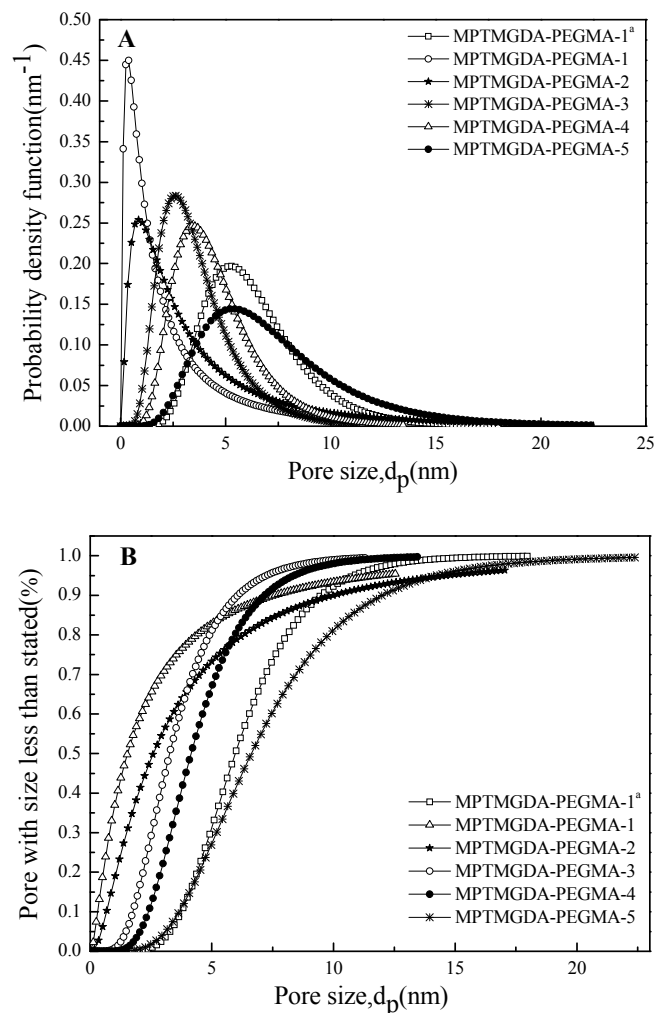


Fig. 9 (a) Probability density function curves; and (b) pore with size less than stated curves of PVDF-PTMGDA-PEGMA membranes

Table 4 The mean effective pore size and molecular weight cut-off (MWCO) of PVDF-PTMGDA-PEGMA membranes

Membrane no.	d_p (nm)	MWCO (Da)
MPTMGDA-PEGMA-0	10.70	35800
MPTMGDA-PEGMA-1 ^a	9.50	25300
MPTMGDA-PEGMA-1	6.08	11400
MPTMGDA-PEGMA-2	7.18	15300
MPTMGDA-PEGMA-3	7.58	16900
MPTMGDA-PEGMA-4	10.00	27800
MPTMGDA-PEGMA-5	12.01	38700

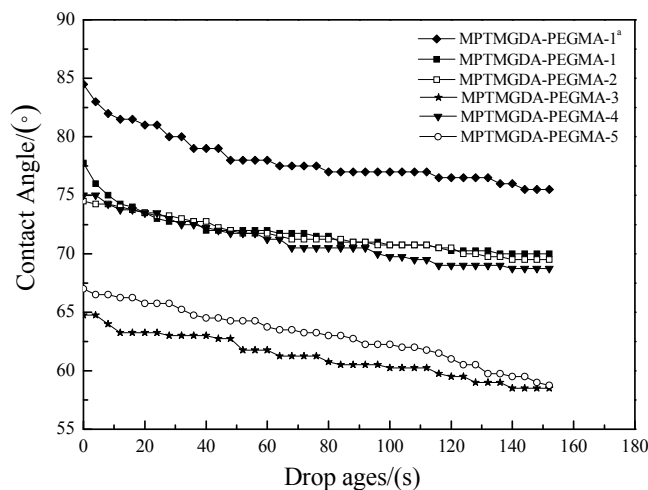


Fig. 10 The dynamic contact angles of PVDF-PTMGDA-PEGMA membranes

mean effective pore size from 6.08 nm to 12.01 nm. Furthermore, the variation of MWCO values was similar to the mean effective pore size. Table 4 revealed that the MWCO value initially decreased from 25300 Da to 11400 Da and then subsequently increased to 38700 Da.

3.6 Dynamic Contact Angle (DCA)

The pure water contact angle of membrane surface was often used to describe the hydrophilicity of membranes. The dynamic contact angles of the PVDF-PTMGDA-PEGMA membranes are presented in Fig. 9. The dynamic contact angle of the pure PVDF membrane and MPTMGDA-PEGMA-1^a were high. The reason for this was that there was no surface segregation of the hydrophilic segment during demixing process. However, the hydrophilicity of the membranes fabricated via in situ free radical polymerization improved, and the contact angle declined linearly with time. The hydrophilicity further improved with the increasing content of the dopants. This confirmed the surface segregation of the hydrophilic segment during demixing process, which was consistent with the permeability results. And due to the hydrophilic segment-rich part of the membrane surface with the increase concentration of the dopants, the contact angle declined linearly.

4. Conclusions

By the introduction of a hydrophobic PTMGDA to in situ free radical polymerization system of PVDF/PTMGDA/PEGMA/TEP/DMAc, the performances of resultant membrane were improved greatly. With the existence of the dopants, the water flux increased to 60 L.m⁻¹.h⁻¹ and the flux recovery rate enhanced 47.9%. As the increasing concentration of the PTMGDA/PEGMA dopants, the surface tension and the precipitation rate of the casting solution decreased, whereas, the viscosity increased. The PVDF-PTMGDA-PEGMA membrane demonstrated improved hydrophilicity, excellent mechanical properties, increased the mean effective pore size and enhanced permeability properties.

Acknowledgments

The authors are thankful for the financial support received from the National Natural Science Foundation of China (51172144), Shanghai Union Program (LM201249), Special Project of the Development and Industrialization of New Materials of National Development and Reform Commission in China (20132548), the Key Technology R&D Program of Shanghai Committee of Science and Technology in China (13521102000 and 14231201503) and the Key Technology R&D Program of Jiangsu Committee of Science and Technology in China (BE2013031).

References

- Awanis Hashim, N., Liu, F., Moghareh Abed, M.R. and Li, K. (2012), "Chemistry in spinning solutions: Surface modification of PVDF membranes during phase inversion", *J. Membr. Sci.*, **415-416**, 399-411.
- Boributh, S., Chanachai, A. and Jiratananon, R. (2009), "Modification of PVDF membrane by chitosan solution for reducing protein fouling", *J. Membr. Sci.*, **342**(1-2), 97-104.
- Chen, G.E., Wu, W.Z., Zhang, P.Y. and Xu, Z.L. (2014), "Influence of residence time on performances of PVDF membranes", *J. Appl. Polym. Sci.*, **131**.
- Cui, Z., Drioli, E. and Lee, Y.M. (2014), "Recent progress in fluoropolymers for membranes", *Prog. Polym. Sci.*, **39**(1), 164-198.
- Forsythe, J.S. and Hill, D.J.T. (2000), "The radiation chemistry of fluoropolymers", *Prog. Polym. Sci.*, **25**(1), 101-136.
- Hester, J.F., Banerjee, P. and Mayes, A.M. (1999), "Preparation of protein-resistant surfaces on poly(vinylidene fluoride) membranes via surface segregation", *Macromolecules*, **32**(5), 1643-1650.
- Katsoufidou, K., Yiantsios, S.G. and Karabelas, A.J. (2005), "A study of ultrafiltration membrane fouling by humic acids and flux recovery by backwashing: Experiments and modeling", *J. Membr. Sci.*, **266**(1-2), 40-50.
- Khayet, M., Feng, C.Y., Khalbe, K.C. and Matsuura, T. (2002), "Preparation and characterization of polyvinylidene fluoride hollow fiber membrane for ultrafiltration", *Polymer*, **43**, 3879-3890.
- Kim, Y., Rana, D., Matsuura, T. and Chung, W.-J. (2009), "Influence of surface modifying macromolecules on the surface properties of poly(ether sulfone) ultra-filtration membranes", *J. Membr. Sci.*, **338**(1-2), 84-91.
- Letchford, K. and Burt, H. (2007), "A review of the formation and classification of amphiphilic block copolymer nanoparticulate structures: Micelles, nanospheres, nanocapsules and polymersomes", *Eur. J. Pharm. Biopharm.*, **65**(3), 259-269.
- Li, J.H., Li, M.Z., Jing, M., Wang, J.B., Shao, X.S. and Zhang, Q.Q. (2012), "Improved surface property of PVDF membrane with amphiphilic zwitterionic copolymer as membrane additive", *Appl. Surf. Sci.*, **258**(17), 6398-6405.
- Li, J.-H., Shao, X.S., Zhou, Q., Li, M.Z. and Zhang, Q.Q. (2013), "The double effects of silver nanoparticles on the PVDF membrane: Surface hydrophilicity and antifouling performance", *Appl. Surf. Sci.*, **265**, 663-670.
- Liu, F., Xu, Y.Y., Zhu, B.K., Zhang, F. and Zhu, L.P. (2009), "Preparation of hydrophilic and fouling resistant poly(vinylidene fluoride) hollow fiber membranes", *J. Membr. Sci.*, **345**(1-2), 331-339.
- Liu, F., Hashim, N.A., Liu, Y., Moghareh Abed, M.R. and Li, K. (2011), "Progress in the production and modification of PVDF membranes", *J. Membr. Sci.*, **375**(1-2), 1-27.
- Liu, B., Chen, C., Li, T., Crittenden, J. and Chen, Y. (2013a), "High performance ultrafiltration membrane composed of PVDF blended with its derivative copolymer PVDF-g-PEGMA", *J. Membr. Sci.*, **445**, 66-75.
- Liu, M., Wei, Y.M., Xu, Z.L., Guo, R.Q. and Zhao, L.B. (2013b), "Preparation and characterization of polyethersulfone microporous membrane via thermally induced phase separation with low critical solution temperature system", *J. Membr. Sci.*, **437**, 169-178.
- Loh, C.H., Wang, R., Shi, L. and Fane, A.G. (2011), "Fabrication of high performance polyethersulfone UF

- hollow fiber membranes using amphiphilic Pluronic block copolymers as pore-forming additives”, *J. Membr. Sci.*, **380**(1-2), 114-123.
- Neugebauer, D. (2007), “Graft copolymers with poly(ethylene oxide) segments”, *Polym. Int.*, **56**(12), 1469-1498.
- Prince, J.A., Rana, D., Singh, G., Matsuura, T., Jun Kai, T. and Shanmugasundaram, T.S. (2014), “Effect of hydrophobic surface modifying macromolecules on differently produced PVDF membranes for direct contact membrane distillation”, *Chem. Eng. J.*, **242**, 387-396.
- Shi, L., Wang, R., Cao, Y., Liang, D.T. and Tay, J.H. (2008), “Effect of additives on the fabrication of poly(vinylidene fluoride-co-hexafluoropropylene) (PVDF-HFP) asymmetric microporous hollow fiber membranes”, *J. Membr. Sci.*, **315**(1-2), 195-204.
- Ulbricht, M. and Belfort, G. (1996), “Surface modification of ultrafiltration membranes by low temperature plasma. II. Graft polymerization onto polyacrylonitrile and polysulfone”, *J. Membr. Sci.*, **111**(2), 193-215.
- Vähä-Nissi, M., Kauppi, E., Sahagian, K., Johansson, L.S., Peresin, M.S., Sievänen, J. and Harlin, A. (2012), “Growth of thin Al₂O₃ films on biaxially oriented polymer films by atomic layer deposition”, *Thin Solid Films.*, **522**, 50-57.
- Wang, P., Tan, K.L., Kang, E.T. and Neoh, K.G. (2002), “Plasma-induced immobilization of poly(ethylene glycol) onto poly(vinylidene fluoride) microporous membrane”, *J. Membr. Sci.*, **195**(1), 103-114.
- Yadav, S.K., Mahapatra, S.S., Cho, J.W., Park, H.C. and Lee, J.Y. (2010), “Enhanced mechanical and dielectric properties of poly(vinylidene fluoride)/polyurethane/multi-walled carbon nanotube nanocomposites”, *Fiber. Polym.*, **10**(6), 756-760.
- Yang, Q., Kang, X.Z., Wei, D.Z., Li, W.J. and Ulbricht, M. (2005), “Surface modification of polypropylene microporous membranes with a novel glycopolymer”, *Chem. Mat.*, **17**(11), 3050-3058.
- Yang, Q., Chung, T.S. and Santoso, Y.E. (2007), “Tailoring pore size and pore size distribution of kidney dialysis hollow fiber membranes via dual-bath coagulation approach”, *J. Membr. Sci.*, **290**(1-2), 153-163.
- Yu, L.Y., Xu, Z.L., Shen, H.M. and Yang, H. (2009), “Preparation and characterization of PVDF-SiO₂ composite hollow fiber UF membrane by sol-gel method”, *J. Membr. Sci.*, **337**(1-2), 257-265.
- Yuan, G., Xu, G., Ji, C. and Wei, Y. (2008), “Study on diffusion-limited and reaction aggregation dynamics model in PVDF membrane formation process by NIPS method”, *Membr. Sci. Tech.*, **30**, 26 p.
- Zhang, W., Shi, L., An, Y., Gao, L., Wu, K. and Ma, R. (2004), “A Convenient Method of Tuning Amphiphilic Block Copolymer Micellar Morphology”, *Macromolecules*, **37**(7), 2551-2555.
- Zhang, M., Nguyen, Q.T. and Ping, Z. (2009), “Hydrophilic modification of poly(vinylidene fluoride) microporous membrane”, *J. Membr. Sci.*, **327**(1-2), 78-86.
- Zhang, P.Y., Xu, Z.L., Yang, H., Wei, Y.M. and Wu, W.Z. (2013a), “Fabrication and characterization of PVDF membranes via an in situ free radical polymerization method”, *Chem. Eng. Sci.*, **97**, 296-308.
- Zhang, P.Y., Xu, Z.L., Yang, H., Wei, Y.M., Wu, W.Z. and Chen, D.G. (2013b), “Preparation and characterization of PVDF-P(PEGMA-r-MMA) ultrafiltration blend membranes via simplified blend method”, *Desalination*, **319**, 47-59.
- Zhang, P.Y., Yang, H., Xu, Z.L., Wei, Y.M., Guo, J.L. and Chen, D.G. (2013c), “Characterization and preparation of poly(vinylidene fluoride) (PVDF) microporous membranes with interconnected bicontinuous structures via non-solvent induced phase separation (NIPS)”, *J. Polym. Res.*, **20**(2), 66-78.
- Zhang, P.Y., Yang, H. and Xu, Z.L. (2012), “Preparation of Polyvinylidene Fluoride (PVDF) Membranes via Nonsolvent Induced Phase Separation Process using a Tween 80 and H₂O Mixture As an Additive”, *Ind. Eng. Chem. Res.*, **51**(11), 4388-4396.
- Zhang, P.Y., Xu, Z.L., Yang, H., Wei, Y.M. and Wu, W.Z. (2013), “Fabrication and characterization of PVDF membranes via an in situ free radical polymerization method”, *Chem. Eng. Sci.*, **97**, 296-308.
- Zhao, L.B., Xu, Z.L., Liu, M. and Wei, Y.M. (2014), “Preparation and characterization of PSf hollow fiber membrane from PSf-HBPE-PEG400-NMP dope solution”, *J. Membr. Sci.*, **454**, 184-192.
- Zuo, G. and Wang, R. (2013), “Novel membrane surface modification to enhance anti-oil fouling property for membrane distillation application”, *J. Membr. Sci.*, **447**, 26-35.